Available online at www.sciencedirect.com
SCIENCE DIRECT®
Journal of Sound and Vibration 288 (2005) 91–106
JOURNAL OF SOUND AND VIBRATION
www.elsevier.com/locate/jsvi

Features of blast-induced vibration source and identification of geostructures

H. Ding[a,*], R. Labbas[b], Z.M. Zheng[a]

[a]*Division of Engineering Sciences, Institute of Mechanics, CAS, Beijing 100080, China*
[b]*Mathematical Laboratory, Universite du Havre, LMAH, F.S.T., BP 540, 25 rue Philippe Lebon, F-76058 Le Havre Cedex, France*

Received 22 December 2003; received in revised form 26 July 2004; accepted 20 December 2004
Available online 8 March 2005

Abstract

An analysis of the behavior of spherical elastic wave radiation from an impulsively loaded cavity embedded in an infinite space has been carried out. It is confirmed that the propagating waveform is dominated by the natural vibration mode of the cavity and the magnitude of the dominant response depends only on the impulse of the time function of the load, and not the profile of the time function. This finding supports the fact that the dynamic signals recoded away from the blasting explosive contain mainly the characteristics of the natural vibrations of the geological structures near the cavity created by a blast. Based on this finding, two promising methods are proposed for the identification of geo-structures and parameters.

1. Introduction

Elastic waves have been used for a long time in applications in geophysics, seismology, earth exploration, and non-destructive evaluation of materials and structures [1]. With the help of advanced computational inverse techniques [2,3], systematic procedures can be developed for quantitatively determining the parameters (dimensions, material properties, parameterized

*Corresponding author. Tel.: +86 1 62657887; fax: +86 1 62561284.
E-mail addresses: hding@imech.ac.cn (H. Ding), labbas@univ-lehavre.fr (R. Labbas), zhengzm@imech.ac.cn (Z.M. Zheng).

0022-460X/$ - see front matter © 2005 Elsevier Ltd. All rights reserved.
doi:10.1016/j.jsv.2004.12.017

Nomenclature

λ, μ	Lame's constants of elastic material	ω	characteristic circular frequency of the cavity $\left(=(1/T_0)\sqrt{1-\xi^2}\right)$
ρ	density of material	a	decaying parameter of the cavity $(=\xi/T_0)$
c_p	longitudinal wave speed	I	impulse of the excitation load
c_s	transverse wave speed	T	duration of the excitation load
ξ	ratio of wave speeds $(=c_s/c_p)$	η	relative ratio between the duration of excitation load and the characteristic time of the cavity $(=T/T_0)$
r_0	radius of an embedded cavity		
T_0	characteristic time of the cavity $(=r_0/2c_s)$	γ	dimensionless time variable $(=t/T)$

configurations, etc.) of the systems [4–10], geometries of structural configurations [11–15], and profiles of wave sources and loadings [16]. For effective inverse analyses or identification of any system, a good understanding of the features of wave response is essential. This paper aims to reveal some of the important features of the wave response to the explosive loading by analyzing the wave response to the impulsive loading applied in cavity embedded in infinite elastic media.

Estimation of blasting waves plays an important role in safety evaluations of engineering blasting and in the prediction of geophysical structures. The importance of the studies on the sources of blasting vibration has been recognized since the very beginning of the research works, as mentioned by Sharpe [17], "of the three physical processes involved in seismic exploration, namely the initiation of the seismic waves, their propagation, reflection, refraction, and dispersion, and the recording of some form of the motion of the surface, we possess the east satisfactory understanding of the initiation process". Although many theoretical models have been established [18–25], due to the extreme complexities of real site conditions, the practical estimations are usually based on some empirical or semi-empirical methods ([26–30], etc.). With the development of the measurement and computational techniques as well as the computer technologies, it is possible to go beyond some empirical and simple analytical results and to obtain a more accurate description of blast-induced vibrations under real conditions. More importantly, a better understanding is required on the main source and propagation features of the blasting wave, because it allows one to overcome the difficulty of the limitation of the site data and to extract the most important factors from extremely complex real site conditions.

In seismic studies (on natural earthquakes and blast-induced quakes), the seismic source has long been assumed as a point source moment, whose time function is determined from the far-field waveform and its spectrum features [20]. The inverse problem of the seismic source becomes the determination of the form of the point moment and its time function. Of course, the equivalent cavity theory developed in early times [17–19] is also an efficient source model for blasting waves. However, with its lack of different kinds of load models and lack of studies on the time functions, it has not drawn enough attention by researchers recently. The semi-empirical method based on the source scaling and wavelet deconvolution has also attracted researchers [26,27]. The development of numerical methods [21,31] in this field has always been a challenge due to the inherently complicated properties of rock mass, blasting process, and highly nonlinear and strain rate-dependent dynamic responses.

As the point source moment takes the form of a spatial divergence in the equilibrium equations and the non-smoothness of the derivative of Dirac function, in the best case, is in $H^{-2-\varepsilon}(\Omega)(\varepsilon>0)$ space (the dual space of Sobolev Space $H^{2+\varepsilon}(\Omega)$, where $H^{2+\varepsilon}(\Omega)$ is the space of functions and its derivatives of order less than $2+\varepsilon$ are square integrable in the domain Ω [32]), the best smoothness of the solution of the dynamic linear elastic equations under the action of the point source moment is in the space $H^2(t;H^{-2-\varepsilon})\cap L^2(t;H^{-\varepsilon})$. This implies that the solution corresponding to the action of the point source moment is a generalized function, which cannot be defined in a point-to-point manner, but as a functional. Therefore, it may be concluded that the analytical solution of the point source moment is singular, resulting in the appearance of components of infinitely high frequencies. In other words, these components of high frequencies come from the spatial singularities of the load. Therefore, if we do not limit the frequency range, a waveform with a limited bandwidth cannot be obtained. This is why people have to limit the bandwidth in applying a point source moment.

Due to simplicity, the cavity theory gives some explicit results revealing the features of blasting waves. Using numerical methods, results for cavities of different shapes can also be obtained. However, for quantitative determinations of the cavity shape, size, and the applied load model, time function, there exists no suitable theory or rule.

A reliable numerical model validated against field measured data, will provide a cost-effective means of examining the blasting wave propagation in engineering systems. Since rock damage and stress wave propagation are highly dependent on material properties and explosion process, it is necessary to properly model the explosion process, effects of existing discontinuities in rock mass, cumulative damage of rock mass caused by blasting loads, degradation of stiffness and strength and plastic deformations of rock material, wave speeds and attenuation properties, etc. With the complexity of site conditions, it is nearly impossible to handle all these factors without simplification. In practice, either semi-empirical equivalent source models or equivalent material approaches are used to simplify the situations. The better the understanding of physical laws governing the process in blasting vibration we get, the more accurate simulation we shall make.

It is known that, in a process of fragmenting blasting, the charge may be regarded as an impulsive load of very short time duration acting on the surrounding media. The energy released by the charge is mainly transferred to the surrounding media through this impulse load, resulting in deformation, damage and movement of the media. Obviously, the impulse load has not been transferred in a form of sharp impulse, but rather propagated outward through the filtering of the surrounding media. Many researchers believed that the filtering mainly depends on the inelastic properties of the media (such as plasticity, damping, etc.). Recently, Ding and Zheng [33] have developed a new source model for blasting vibration which combines the cavity theory and the moment tensor representation. The model is especially established for numerical purpose, and the numerical results have shown a good accordance with the experimental data. The physical mechanism for the model is based on the fact that the propagating wave signal mainly comes from the natural vibration of the geophysical structure after blasting. This fact not only reveals the physics in the process of blasting vibration but is also applicable to engineering problems in geophysics, such as the identification of weak layers and the determination of the macroscopic material strength of rock.

In this paper, the fact observed by Ding and Zheng will be again revealed by analyzing the asymptotic behaviors of the spherical elastic wave radiation from an impulsively loaded cavity. Applications of these important facts to engineering geophysics will also be discussed.

2. Analysis of elastic wave radiation

Consider an infinite media with a spherical cavity of elastic material defined by $r \geqslant r_0$ in a spherical coordinate system with the origin at the center of the cavity. The elastic media is loaded by a uniform pressure $P(t)$ at the cavity's boundary defined by $r = r_0$. Due to spherical polar symmetry, all field variables depend only on the radial distance r and time t. The displacement is in the radial direction only and is denoted by $u(r, t)$. The solution $u(r, t)$ is given by (see the appendix)

$$u = \frac{\partial \phi}{\partial r} \tag{1}$$

with

$$\phi(r, t) = \frac{1}{r} f\left(t - \frac{r - r_0}{c_p}\right) \tag{2}$$

and

$$f(t) = \mathrm{e}^{-at}(A \cos t(\omega t) + B \sin t(\omega t)) + f_p(t), \tag{3}$$

$$f_p(t) = \mathrm{e}^{-at}(g_1(t) \cos(\omega t) + g_2(t) \sin(\omega t)), \tag{4}$$

$$g_1(t) = \frac{r_0 c_s^2}{\mu \omega} \int_0^t \mathrm{e}^{as} \sin(\omega s) P(s)\, \mathrm{d}s, \tag{5}$$

$$g_2(t) = \frac{r_0 c_s^2}{\mu \omega} \int_0^t \mathrm{e}^{as} \cos(\omega s) P(s)\, \mathrm{d}s. \tag{6}$$

As the duration of blasting load is very short, an asymptotic approximation of the solution $f(t)$ given by Eq. (3) can be made as follows. Suppose that the pressure can be written in the form of

$$P(t) = I \rho_T(t), \tag{7}$$

in which I is the impulse of the load, and

$$\rho_T(t) = \frac{1}{T} \rho(t/T) \tag{8}$$

is an arbitrary dimensionless function, and $\rho(t)$ satisfies

$$\rho(t) = 0 \ \text{ for } t > 1 \quad \text{and} \quad \int \rho\, \mathrm{d}t = 1, \ \rho(0+) = 0. \tag{9}$$

It is seen that $P(t)$ has a constant impulse I for different duration T of time. The assumption $\rho(0+) = 0$ implies that the initial jump of the applied load is zero. For fragmenting blasting, the shock wave is smoothed by the inelastic material properties in the damaged region; therefore this

assumption of zero initial jump is correct for pressure caused fragmenting blasting. Under this assumption, we have

$$f(t) = f_p(t). \tag{10}$$

For an excitation of the form (7), we let

$$\eta = \frac{T}{T_0}. \tag{11}$$

Then for very short-time excitation duration T (compared with the characteristic time T_0 that is related to the cavity size (see the appendix)), η should be very small. Solution $f_p(t)$ can be approximated in the following asymptotic form:

$$f_p(t) = f_0(t) + O(\eta), \tag{12}$$

where the dominant term

$$f_0(t) = -\frac{r_0 c_s^2}{\omega\mu} I \mathrm{e}^{-at} \sin \omega t \tag{13}$$

depends only on the impulse of the load, and does not depend on the form of the time function $\rho(t)$. The dominant term contains the natural vibration mode of the cavity. Therefore, it is found that the response to short-time excitation is dominated by the natural vibration mode. To obtain expression (12), we first make a change of variable

$$\gamma = \frac{t}{T}. \tag{14}$$

Then we use the Taylor's expansion of functions

$$\mathrm{e}^x = 1 + O(x), \tag{15}$$

and

$$\cos(x) = 1 + O(x^2), \tag{16}$$

$$\sin(x) = x + O(x^3) \tag{17}$$

to approximate the integrands in Eqs. (5) and (6), which can be expressed as

$$\begin{aligned} -\frac{g_1(t)}{I} &= \Lambda \int_0^{t/T} \mathrm{e}^{\eta\xi\gamma} \sin(\eta\beta\gamma)\rho(\gamma)\,\mathrm{d}\gamma \\ &= \Lambda \int_0^{t/T} (1 + O(\eta))(\eta\beta\gamma + O(\eta^3))\rho(\gamma)\,\mathrm{d}\gamma \\ &= \Lambda O(\eta) \int_0^{t/T} \rho(\gamma)\,\mathrm{d}\gamma = O(\eta), \end{aligned} \tag{18}$$

$$-\frac{g_2(t)}{I} = \Lambda \int_0^{t/T} e^{\eta\xi\gamma} \cos(\eta\beta\gamma)\rho(\gamma)\,d\gamma$$
$$= \Lambda \int_0^{t/T} (1 + O(\eta))(1 + O(\eta^2))\rho(\gamma)\,d\gamma$$
$$= \Lambda \int_0^{t/T} \rho(\gamma)\,d\gamma + O(\eta), \tag{19}$$

in which

$$\Lambda = \frac{r_0 c_s^2}{\omega\mu} \quad \text{and} \quad \beta = \sqrt{1-\xi^2}, \tag{20}$$

For $t \geqslant T$, Eq. (19) gives

$$g_2(t) = -\Lambda I \int_0^1 \rho(\gamma)\,d\gamma + O(\eta) = \Lambda + O(\eta) \tag{21}$$

and for $t < T$, we have

$$\sin(\omega t) = (\eta\beta\gamma + O(\eta^3)) = O(\eta). \tag{22}$$

Estimates (18), (21), (22) and (4) lead to the asymptotic expansion (12).

An example is given in the following to show the contrast of $f(t)$ with its dominant term $f_0(t)$ for different time duration ratios η.

Let $\theta = t/T_0$ and $\theta_T = T/T_0$, taking a special form of $\rho(t)$,

$$\rho(t) = \begin{cases} 1, & t \in [0,1], \\ 0 & \text{otherwise.} \end{cases} \tag{23}$$

Note here that for simplicity we chose the above form of rectangular pulse for $\rho(t)$, where $\rho(0+) \neq 0$. However, this does not affect the findings given in the following, as one can approximate function (23) by a smooth function with zero initial jump and this approximation does converge for $f(t)$ and its first derivative, and the effect of $\rho(0+) \neq 0$ leads only to another term of natural vibration in the solution. Then we get

$$g_1(t) = \frac{\Lambda I}{\theta_T} \begin{cases} e^{\xi\theta}(\xi \sin(\beta\theta) - \beta\cos(\beta\theta)) + \beta, & t < T, \\ e^{\xi\theta_T}(\xi \sin(\beta\theta_T) - \beta\cos(\beta\theta_T)) + \beta, & t \geqslant T, \end{cases} \tag{24}$$

$$g_2(t) = -\frac{\Lambda I}{\theta_T} \begin{cases} e^{\xi\theta}(\xi \cos(\beta\theta) + \beta\sin(\beta\theta)) - \xi, & t < T, \\ e^{\xi\theta_T}(\xi \cos(\beta\theta_T) + \beta\sin(\beta\theta_T)) - \xi, & t \geqslant T. \end{cases} \tag{25}$$

Normalizing $f_p(t)$ by ΛI gives

$$F(t) = \frac{f_p(t)}{\Lambda I} = G_1(t)e^{-\xi\theta}\cos(\beta\theta) + G_2(t)e^{-\xi\theta}\sin(\beta\theta), \tag{26}$$

in which

$$G_1(t) = \frac{1}{\theta_T}\begin{cases} e^{\xi\theta}(\xi\sin(\beta\theta) - \beta\cos(\beta\theta)) + \beta, & t < T, \\ e^{\xi\theta_T}(\xi\sin(\beta\theta_T) - \beta\cos(\beta\theta_T)) + \beta, & t \geqslant T, \end{cases} \tag{27}$$

$$G_2(t) = -\frac{1}{\theta_T}\begin{cases} e^{\xi\theta}(\xi\cos(\beta\theta) + \beta\sin(\beta\theta)) - \xi, & t < T, \\ e^{\xi\theta_T}(\xi\cos(\beta\theta_T) + \beta\sin(\beta\theta_T)) - \xi, & t \geqslant T \end{cases} \tag{28}$$

and the normalized dominant part is given by

$$F_0(t) = \frac{f_0(t)}{\Lambda I} = -e^{-\xi\theta}\sin(\beta\theta). \tag{29}$$

Fig. 1 shows the comparisons of $F(t)$ with its dominant part $F_0(t)$ for different time ratio η.

From the figure, it can be seen that for short excitation, the response $F(t)$ is very close to its asymptotic approximation, i.e. the dominant part $F_0(t)$.

Since we do not have experimental data for the estimation of η, some reference data are hence used to give some approximate bounds of it. From the experimental results of [30], the characteristic time of the blasted cavity could be estimated as (using $T_0 = (1/\omega)\sqrt{1-\xi^2}, \xi^2 = \frac{3}{8}$)

$$\frac{T_0}{Q^{1/3}} = 6.4\,\mathrm{ms/kg^{1/3}} \tag{30}$$

From the experimental results of [34], the duration of the stress wave near the blasted region could be estimated as

$$\frac{T_0}{Q^{1/3}} = \begin{cases} 0.35\,\mathrm{ms/kg^{1/3}} & \text{for saturated situation,} \\ 3.2\,\mathrm{ms/kg^{1/3}} & \text{for dry situation.} \end{cases} \tag{31}$$

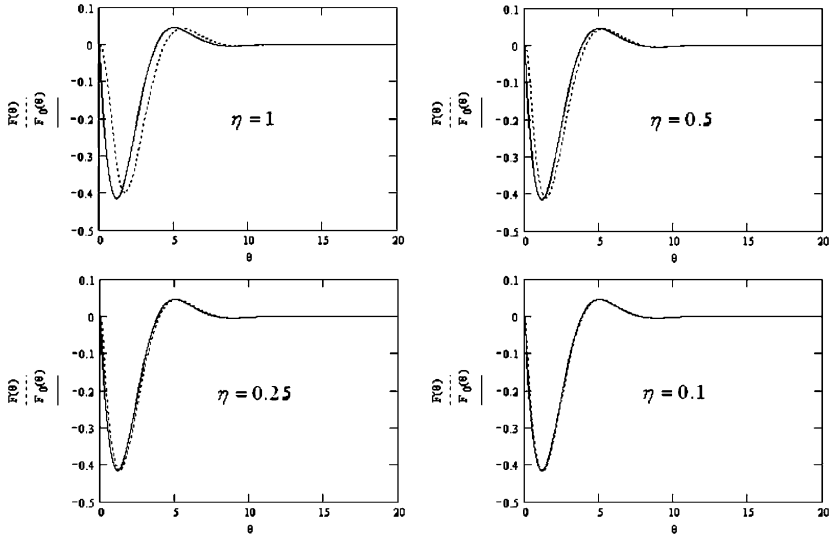

Fig. 1. Comparisons of $F(t)$ with its dominant part $F_0(t)$ for different time ratio η.

The experimental results given by Sun are in the condition between saturated situation and dry situation, and hence the maximum value of η should be between 0.05 and 0.53. In practice, for fragmenting blasting it is believed that $\eta \leqslant 0.25$, and therefore the far-field signal comes mainly from the dominant part $F_0(t)$, and the wave forms depend only on the geostructure near the blasted region and the properties of the medium in the propagation pass.

3. Applications to engineering problems in geophysics

From the above discussion, we conclude that the vibrating signals recorded away from the blasting explosive contain the characteristics of the natural vibrations of the geological structures near the broken (blasted) region (this is true even for the case that is without the assumption $P(0+) = 0$). For fragmenting blasting, the wave radiated from the blasting should be the emission of the natural vibration mode excited by the impulse load by explosion, like the solution $f_0(t)$. So the equivalent blasting vibration source could be modeled as a distributed moment tensor enclosed in a certain region around the explosive, and the time variation of the moment tensor depends mainly on its impulse. This gives a strong explanation of the findings given in Ref. [33]. From site observation, it is not difficult to obtain the wave speeds and, the main frequency of the wave signals. As the main frequency stays nearly unchanged in a certain range of the propagation pass, it is not affected very much by the propagation pass medium. From this point of view, the characteristic time of the blasting source region, i.e. the period of the main frequency of the blasting vibration, could easily be estimated, and thus the size of the loading region in the source model [33]. Then the moment tensor and the impulsive intensity I of the source model could be determined by an identification process. On the other hand, the mechanism presented in the source model could be used to identify the characteristics of geostructures from observing the data of the blasting wave. Several trial applications are as follows.

3.1. Identification of the strength property of geomaterial

From the analysis in the previous section and the site data, it is strongly suggested that the size of the loading region in the source model is proportional to the main frequency of the wave signal. As the size of the loading region has statistical and integrated information of the strength properties of medium, combining with some other information, we can extract the strength properties of medium from the data of main frequencies of waves from a well-defined test with specified blasting load conditions.

3.2. Identification of thin weak layers and crack

Because the vibration signal retains the characteristics of the natural vibration of the geometrical structure modified by the explosion near the source, we can use explosives sources to identify the thin weak layers in engineering geostructures. Fig. 2 gives a schematic explanation of this method.

We have done some numerical testing to confirm the feasibility of the method. The testing results have been done for a weak layer placing under the ground surface at depth.

Numerical simulations have been done for a model as shown in Fig. 3. The block has a dimension of 41 m × 41 m × 41 m. The horizontal weak layers centers are under the ground surface at a depth of 30.5 m, and with the thickness of 1 m and different dimensions (10 m, 22 m, 34 m, etc.). Blasting sources are placed along the vertical central line of this block with different depths. LS_DYNA with the source model of blasting vibration proposed by [33] is used to perform the numerical tests, the moment tensor is isotropic in a 1 m × 1 m × 1 m region and the time function is of the form of an isosceles triangle with constant area (constant impulse) for all numerical tests. All media are supposed to be isotropic and elastic. For solids above and below weak layers, $E = 2.4 \times 10^{10}$, $v = 0.3$, $\rho = 2400$. For weak layers and broken regions, $E = 2.4 \times 10^{8}, v = 0.3, \rho = 2400$. Each face of the block is imposed transmitting boundary conditions but the upper face (ground surface) is stress free. Sensors are installed at points such as A or B on the free surface in the experiment to pick up blasting vibration signals. The position of A or B on the free surface does not affect the qualitative effects of the results, so for the following, the position of A or B will not be mentioned.

Fig. 4 shows the comparison of the numerical results for cases with weak layer and without weak layer when the explosive is placed in the weak layer. And Fig. 5 shows the comparison of the numerical results for cases with weak layer and without weak layer when the explosive is placed in the position near the ground surface (1.5 m below the free surface).

From the results, we could find that when the explosive is placed in the position near the ground surface, the existence of the weak layer does not affect strongly the observed signal at the ground surface (see Fig. 5). But in contrast, when the explosive is placed in the position near the weak layer, the characteristics of the signal are totally different (see Fig. 4). The signal reflects the information of the weak layer. As the constant source's impulse and the isotropic moment tensor with a constant region have been used for all calculations, the results need some comments: in general, for different material, the region occupied by the moment tensor will be different, and the

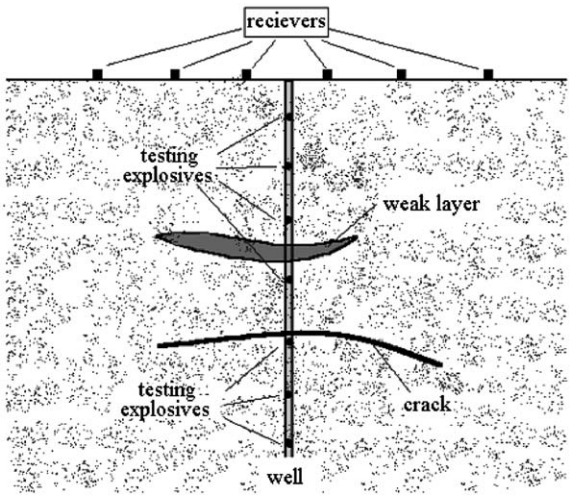

Fig. 2. Schematic explanations of the method to identify the thin weak layers and cracks in engineering geostructures.

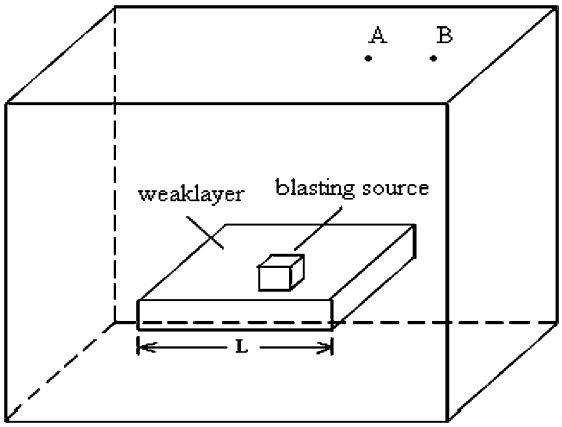

Fig. 3. Numerical model for horizontal weak layers.

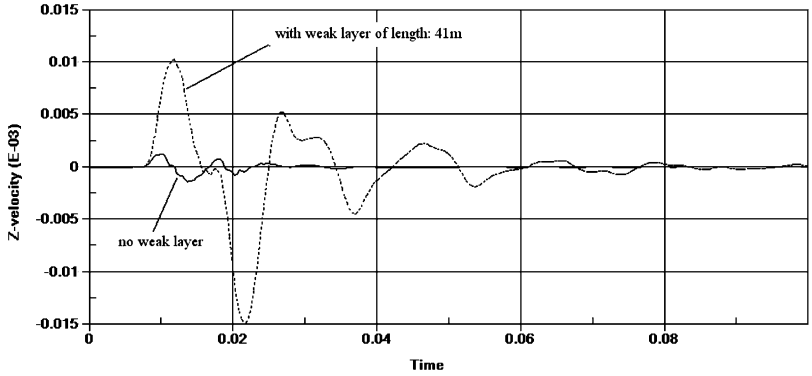

Fig. 4. Comparison of the wave forms with and without weak layer when the explosive is placed in the same position which is near the layer when the layer exists.

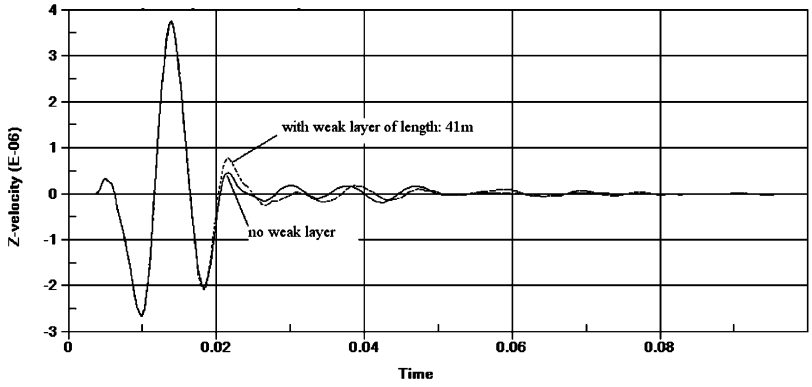

Fig. 5. Comparison of the wave forms with and without weak layer when the explosive is placed in the same position near the ground surface.

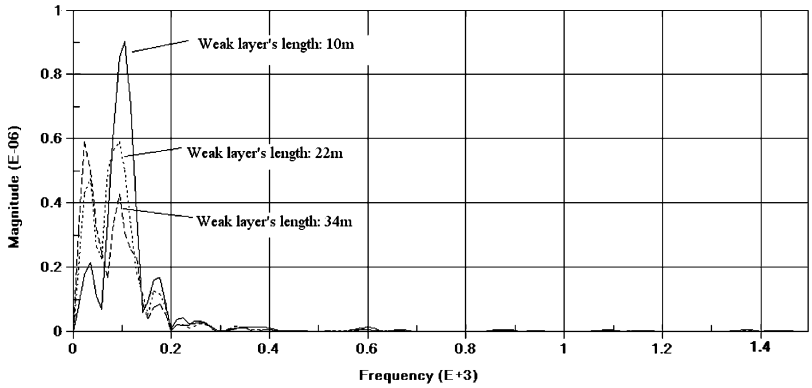

Fig. 6. The numerical results for different lengths of the weak layer in the frequency domain.

weaker the material is, the larger the region will be; the variation of the impulse will be in an inverse manner. As the main frequency of the signal depends on the dimension of the region occupied by the moment tensor, for the real case, the contrast in frequency should be more important than the calculated results. And for the real case, the contrast in amplitude should be less than the calculated results. The results for different lengths of weak layer are shown in Fig. 6

It is shown that as the length of the distribution of the weak layer augments, the peaks' positions will all go to the frequency direction, and the lowest frequency peak augments while others decrease. This conclusion should be true for the real case according to the comments given above.

4. Conclusions and discussions

The asymptotic analysis of the wave radiation from a loaded cavity confirms that for short-time excitation, the spectrum of the radiated wavefield will depend on the resonances of the cavity and not on the details of the actual excitation. And the discussion that the time ratio η for experimental data is in general less than 0.25 leads to that for fragmenting blasting; the dynamic signals recoded away from the blasting explosive contain mainly the characteristics of the natural vibrations of the geological structures near the cavity created by a blast.

From the numerical results given in the previous section, we could suggest the obvious contrasts that the vibrations should exhibit when the weak layer exists. The longer the layer length is, the less the characteristic frequencies of the vibration signals will be.

In the numerical simulation, the constant source's impulse and the isotropic moment tensor with a constant region have been used for all calculations. This is just for the qualitative tendency of the phenomena. Anisotropic moment tensor should be used and calibrated by real tests for real applications in combination with other effects of weak layers such as the shallow effect for transmitting waves, and this will be the future work.

Acknowledgements

This work is supported by the Special Funds for Major State Basic Research Project under Grant No. 2002CB412706; and the project: "The crucial mechanical problems in landsliding engineering" of the Chinese Academy of Sciences.

Appendix A. Elastic wave radiation from a loaded cavity

Within the linear elastic zone, at radial distances $r \geqslant r_0$ there is spherical polar symmetry around an origin at the center of the source, and all field variables depend only on the radial distance r and time t. Displacement is in the radial direction only and is denoted by $u(r, t)$. There arc two components of stress, the radial component

$$\sigma_{rr} = (\lambda + 2\mu)\frac{\partial u}{\partial r} + 2\lambda\frac{u}{r} \tag{A.1}$$

and the normal stress in any direction perpendicular to the radius

$$\sigma_{\theta\theta} = \lambda\frac{\partial u}{\partial r} + 2(\lambda + \mu)\frac{u}{r}, \tag{A.2}$$

in which λ and μ are Lame's constants. The linearized equation of motion is (on neglecting body forces)

$$\frac{\partial \sigma_{rr}}{\partial r} + \frac{2(\sigma_{rr} + \sigma_{\theta\theta})}{r} = \rho\frac{\partial^2 u}{\partial t^2}, \tag{A.3}$$

in which ρ is the density. Then

$$\frac{\partial^2 u}{\partial r^2} + \frac{2}{r}\frac{\partial u}{\partial r} - \frac{2}{r^2}u = \frac{1}{c_p}\frac{\partial^2 u}{\partial t^2}, \tag{A.4}$$

in which

$$c_p^2 = (\lambda + 2\mu)/\rho, \tag{A.5}$$

is the dilatational wave speed. It is convenient to express the radial displacement u in terms of the displacement potential ϕ,

$$u = \frac{\partial \phi}{\partial r}, \tag{A.6}$$

for then it can be seen that ϕ must obey the familiar wave equation for spherical waves

$$\frac{\partial^2}{\partial r^2}(r\phi) = \frac{1}{c_p^2}\frac{\partial^2}{\partial t^2}(r\phi). \tag{A.7}$$

Eq. (A.7) has the solution

$$\phi(r, t) = \frac{1}{r}f\left(t - \frac{r - r_0}{c_p}\right), \tag{A.8}$$

where only outgoing waves have been considered and $f(t)$, with dimensions of volume, is known as the volume injection function. This equation is valid throughout the region where the basic equations (A.1)–(A.3) apply, that is for $r \geqslant r_0$ and $t-(r-r_0)/c_p \geqslant 0$. The displacement in this linear region is found from Eq. (A.6)

$$u(r,t) = -\frac{1}{rc_p} f'(\tau) - \frac{1}{r^2} f(\tau), \tag{A.9}$$

where the prime indicates differentiation with respect to the argument, and

$$\tau = t - \frac{r-r_0}{c_p}, \quad \tau \geqslant 0. \tag{A.10}$$

with

$$f(\tau) = 0 \quad \text{for} \quad \tau < 0. \tag{A.11}$$

The radial stresses can be obtained as

$$\sigma_{rr} = \frac{\mu}{c_s^2 r}\left[f''(\tau + \frac{4c_s^2}{rc_p} f'(\tau) + \frac{4c_s^2}{r^2} f(\tau)\right], \tag{A.12}$$

in which c_s is the share wave speed and given by

$$c_s^2 = \mu/\rho. \tag{A.13}$$

Suppose that at the inner boundary of the linear elastic zone, a uniform pressure $P(t)$ is imposed, i.e.

$$\sigma_{rr} = -P(t) \quad \text{for} \quad r = r_0 \tag{A.14}$$

or

$$f''(t) + \frac{4c_s^2}{r_0 c_p} f'(t) + \frac{4c_s^2}{r_0^2} f(t) = -\frac{r_0 c_s^2}{\mu} P(t). \tag{A.15}$$

Eq. (A.15) has solution of the form

$$f(t) = \mathrm{e}^{-at}(A\cos(\omega t) + B\sin(\omega t)) + f_p(t), \tag{A.16}$$

in which $f_p(t)$ is given by

$$f_p(t) = \mathrm{e}^{-at}(g_1(t)\cos(\omega t) + g_2(t)\sin(\omega t)), \tag{A.17}$$

and with

$$g_1(t) = \frac{r_0 c_s^2}{\mu\omega}\int_0^t \mathrm{e}^{as}\sin(\omega s)P(s)\,\mathrm{d}s, \tag{A.18}$$

$$g_2(t) = \frac{r_0 c_s^2}{\mu\omega}\int_0^t \mathrm{e}^{as}\cos(\omega s)P(s)\,\mathrm{d}s, \tag{A.19}$$

$$a = \frac{\xi}{T_0}, \tag{A.20}$$

$$\omega = \frac{1}{T_0}\sqrt{1-\xi^2}, \tag{A.21}$$

$$T_0 = \frac{r_0}{2c_s}, \tag{A.22}$$

$$\xi = \frac{c_s}{c_p}. \tag{A.23}$$

T_0 is the characteristic time of the local geostructure. From Eq. (A.16), we see that the solution is decomposed into two parts: one is due to the natural vibration of the blasted geostructure (around the cavity) with frequency ω and decaying factor e^{-at}, and it is excited by the initial jump of the load $P(t)$, and another is the direct excitation $f_p(t)$ by the load $P(t)$.

Under the initial condition

$$u(r,0) = 0 \quad \text{and} \quad u_t(r,0) = 0 \tag{A.24}$$

or

$$-\frac{1}{r_0 c_p}f'(0) - \frac{1}{r_0^2}f(0) = 0 \quad \text{and} \quad -\frac{1}{r_0 c_p}f''(0) - \frac{1}{r_0^2}f'(0) = 0, \tag{A.24′}$$

we have

$$A = A(\xi)\frac{r_0^3}{4\mu}P(0) \quad \text{and} \quad B = B(\xi)\frac{r_0^3}{4\mu}P(0) \tag{A.25}$$

with

$$A(\xi) = \frac{2\xi B(\xi)}{2\xi^2 - 1}, \tag{A.26}$$

$$B(\xi) = \frac{1}{\sqrt{1-\xi^2}(2\xi(\frac{3}{2} - 2\xi^2)/(2\xi^2 - 1) + (4\xi^2 - 1)/(2\xi))}. \tag{A.27}$$

From Eq. (A.25), the amplitude of the natural vibration mode is proportional to the initial jump of the applied load. But, in the elastic zone boundary, this jump is generally equal to zero, due to deformation and medium damping.

References

[1] G.R. Liu, Z.C. Xi, *Elastic Waves in Anisotropic Laminates*, CRC Press, Boca Raton, FL, 2001.
[2] G.R. Liu, Y.G. Xu, Z.P. Wu, Total solution for structural mechanics problems, *Computer Methods in Applied Mechanics and Engineering* 191 (2001) 989–1012.
[3] G.R. Liu, X. Han, *Computational Inverse Techniques in Nondestructive Evaluation*, CRC Press, Boca Raton, FL, 2003.
[4] X. Han, G.R. Liu, K.Y. Lam, A quadratic layer element for analyzing stress waves in FGMs and its application in material characterization, *Journal of Sound and Vibration* 236 (2) (2000) 307–321.
[5] G.R. Liu, X. Han, K.Y. Lam, Material characterization of FGM plates using elastic waves and an inverse procedure, *Journal of Composite Materials* 35 (2001) 954–971.

[6] G.R. Liu, X. Han, Y.G. Xu, K.Y. Lam, Material characterization of functionally graded material by means of elastic waves and a progressive-learning neural network, *Composites Science and Technology* 61 (2001) 1401–1411.
[7] G.R. Liu, X. Han, K.Y. Lam, A combined genetic algorithm and nonlinear least squares method for material characterization using elastic waves, *Computer Methods in Applied Mechanics and Engineering* 191 (2002) 1909–1921.
[8] G.R. Liu, X. Han, K.Y. Lam, Determination of elastic constants of anisotropic laminated plates using elastic waves and a progressive neural network, *Journal of Sound and Vibration* 252 (2) (2002) 239–259.
[9] G.R. Liu, W.B. Ma, X. Han, An inverse procedure for determination of material constants of composite laminates using elastic waves, *Computer Methods in Applied Mechanics and Engineering* 191 (2002) 3543–3554.
[10] Y.G. Xu, G.R. Liu, Determination of material properties of multilayered thin films using elastic wave propagation approach, *Journal of Micromechanics and Microengineering* 12 (2002) 723–729.
[11] G.R. Liu, S.C. Chen, Flaw detection in sandwich plates based on time-harmonic response using genetic algorithm, *Computer Methods in Applied Mechanics and Engineering* 190 (42) (2001) 5505–5514.
[12] G.R. Liu, S.C. Chen, A novel technique for inverse identification of distributed stiffness factor in structures, *Journal of Sound and Vibration* 254 (5) (2002) 823–835.
[13] Y.G. Xu, G.R. Liu, Z.P. Wu, X.M. Huang, Adaptive multilayer perceptron networks for detection of cracks in anisotropic laminated plates, *International Journal of Solids and Structures* 38 (2001) 5625–5645.
[14] Y.G. Xu, G.R. Liu, Z.P. Wu, Damage detection for composite plates using lamb waves and projection genetic algorithm, *AIAA Journal* 40 (9) (2002) 1860–1966.
[15] Y.G. Xu, G.R. Liu, Detection of flaws in composite materials from scattered elastic-wave field using modified μGA and gradient-based optimizer, *Computer Methods in Applied Mechanics and Engineering* 191 (2002) 3929–3946.
[16] G.R. Liu, W.B. Ma, X. Han, An inverse procedure for identification of loads on composite laminate plates, *Composite Part B* 33 (2002) 425–432.
[17] J.A. Sharpe, The production of elastic waves by explosion pressure: I—theory and empirical field observations, *Geophysics* 7 (1942) 144–154; II—results of observation near an exploding charge, *Geophysics* 7 (1942) 311–321.
[18] W.I. Duvall, Strain wave shape in rock near explosions, *Geophysics* 18 (2) (1953) 310–323.
[19] R. Favreau, Generation of strain waves in rock by an explosion in a spherical cavity, *Journal of Geophysical Research* 74 (1969) 4267–4280.
[20] B.L.N. Kennett, *Seismic Wave Propagation in Stratified Media*, Cambridge University Press, Cambridge, UK, 1983.
[21] R.L. Gibson, M.N. Toksoz, W.J. Dong, Seismic radiation from explosion loaded cavities in isotropic and transversely isotropic media, *Bulletin of the Seismological Society of America* 86 (6) (1996) 1910–1924.
[22] M.G. Imhof, Multiple multipole expansions for elastic scattering, *Journal of the Acoustical Society of America* 100 (1996) 2969–2979.
[23] M.G. Imhof, Scattering of acoustic and elastic waves using a hybrid multiple multipole expansion-finite element technique, *Journal of the Acoustical Society of America* 100 (1996) 1325–1338.
[24] M. Haartsen, W. Dong, M.N. Toksöz, Dynamic streaming currents from seismic point sources in homogeneous poroelastic media, *Geophysical Journal International* 132 (1998) 256–274.
[25] M.G. Imhof, M.N. Toksöz, The effect of synchronized multiple-cavity sources on seismic radiation, *Bulletin of the Seismological Society of America* 92 (2002) 2381–2390.
[26] A.M. Ziolkowski, W.E. Lerwill, D.W. March, L.G. Peardon, Wavelet deconvolution using a source scaling law, *Geophysical Prospecting* 28 (6) (1980) 872–901.
[27] A.M. Ziolkowski, K. Bokhorst, Determination of the signature of a dynamite source using source scaling: part I: theory, *Geophysics* 58 (8) (1993) 1174–1182; part II: experiment, *Geophysics* 58 (8) (1993) 1183–1194.
[28] R.L. Gibson Jr., W.R. Turpening, A. Born, R.M. Turpening, Observations of borehole source amplitude reduction due to casing, *Geophysical Prospecting* 45 (1997) 1–20.
[29] M.G. Imhof, M.N. Toksöz, Acousto-elastic multiple scattering: a comparison of ultrasonic experiments with multiple multipole expansions, *Journal of the Acoustical Society of America* 101 (1997) 1836–1846.
[30] W.G. Sun, Blasting Quake Sources, Seismic Waves and Their Influences, Ph.D. Thesis, Beijing Institute of Technology, 1998.

[31] H. Hao, C. Wu, Y. Zhou, Numerical analysis of blast-induced stress waves in a rock mass with anisotropic continuum damage models part 1: equivalent material property approach, *Rock Mechanics and Rock Engineering* 35 (2) (2002) 79–94.
[32] H. Ding, Etudes Qualitatives du Comportement d'un Corps Elastique sous l'Effet de Charges Concentrees, Doctoral Thesis, Univ. de Nice, France, September, 1986.
[33] H. Ding, Z.M. Zheng, Source model for blasting vibration, *Science in China, Series E* 45 (4) (2002) 395–407.
[34] J.D. Lin, Stress waves produced by explosions in granite, *Proceedings of the International Symposium on Intense Dynamic Loading and Its Effects (ISIDL, 1986)*, Science Press, Beijing, China, 1986, pp. 282–287.